

# Transcription factor ZBP-89 drives a feedforward loop of $\beta$ -catenin expression in colorectal cancer

<sup>1</sup>Bryan E. Essien\*<sup>#</sup>, <sup>1</sup>Sinju Sundaresan\*, <sup>1</sup>Ramon Ocadiz-Ruiz, <sup>1</sup>Aaron Chavis, <sup>1</sup>Amy C. Tsao, <sup>1</sup>Arthur J. Tessier, <sup>1</sup>Michael M Hayes, <sup>1</sup>Amanda Photenhauer, <sup>1</sup>Milena Saqui-Salces<sup>#</sup>, <sup>1</sup>Anthony J. Kang, <sup>2</sup>Yatrik M. Shah, <sup>3</sup>Balazs Györffy, <sup>1,2</sup>Juanita L. Merchant

<sup>1</sup>Departments of Internal Medicine-Gastroenterology; <sup>2</sup>Molecular and Integrative Physiology, University of Michigan, Ann Arbor, MI; <sup>3</sup>Semmelweis University, <sup>2</sup><sup>nd</sup> Department of Pediatrics, Budapest, Hungary

\*contributed equally

Contact:

Juanita L. Merchant  
109 Zina Pitcher PL  
Ann Arbor, MI 48109-2200  
734-936-6365  
[merchanj@umich.edu](mailto:merchanj@umich.edu)

## **Running Title:**

ZBP-89 Induction of  $\beta$ Catenin Gene Expression

Key Words: transcription; promoter; enteroids; APC; ChIP

The authors have no conflict of interest.

## **Financial Support:**

JM R01 DK55732  
YS R01 CA148828

## **#Current Addresses:**

Bryan Essien, Ph.D.  
Ball State University  
Dept. of Biology (Anatomy & Physiology)  
2000 W University Ave  
Muncie, IN 47306  
[beessien@bsu.edu](mailto:beessien@bsu.edu)

Milena Saquis-Salces, Ph.D.  
University of Minnesota  
Dept of Animal Science  
495K AS/AM;1988 Fitch Ave  
St. Paul, MN 55108-6014

**Abstract:** (248/250)

In colorectal cancer (CRC), APC-mediated induction of unregulated cell growth involves post-translational mechanisms that prevent proteasomal degradation of proto-oncogene  $\beta$ -catenin (CTNNB1) and its eventual translocation to the nucleus. However, about 10 percent of colorectal tumors also exhibit increased CTNNB1 mRNA. Here we show in CRC that increased expression of ZNF148, the gene coding for transcription factor ZBP-89, correlated with reduced patient survival. Tissue arrays showed that ZBP-89 protein was overexpressed in the early stages of CRC. Conditional deletion of Zfp148 in a mouse model of Apc-mediated intestinal polyps demonstrated that ZBP-89 was required for polyp formation due to induction of Ctnnb1 gene expression. CHIP and EMSA identified a ZBP-89 binding site in the proximal promoter of CTNNB1. Recipricolly, siRNA-mediated reduction of CTNNB1 expression also decreased ZBP-89 protein. CHIP identified TCF DNA binding sites in the ZNF148 promoter through which Wnt signaling regulates ZNF148 gene expression. Suppression of either ZNF148 or CTNNB1 reduced colony formation in WNT-dependent, but not WNT-independent cell lines. Therefore, the increase in intracellular  $\beta$ -catenin protein initiated by APC mutations is sustained by ZBP-89-mediated feedforward induction of CTNNB1 mRNA.

## Introduction (5657/5500)

Mutations in the adenomatous polyposis coli gene (*APC*) occur in about 80% of colorectal cancers (CRCs) (1, 2). Most of the mutations prevent interaction with the protein product of the *CTNNB1* locus ( $\beta$ -catenin), which accumulates in the cytoplasm, and then translocates to the nucleus to interact with DNA-binding proteins in the T-cell factor family (LEF/TCF) activating proliferative target genes (2, 3). Although some CRCs exhibit mutations in downstream Wnt target genes, e.g., *AXIN2*, *CCND1*, *MYC*, Wnt-dependent proliferation has been attributed primarily to post-translational alterations that increase  $\beta$ -catenin protein stability. As a result, therapy to disrupt this process has focused on targeting pathways that decrease nuclear  $\beta$ -catenin protein (4). While prior studies have shown increased mRNA expression by in situ hybridization, especially in areas of tissue invasion (5, 6), few proposed therapies focus on regulation of  $\beta$ -catenin gene expression. Recently, it has been shown that thyroid hormone suppresses  $\beta$ -catenin transcription (7). In CRC liver metastases,  $\beta$ -catenin increases its own expression through TCF-4 (8), suggesting that increasing *CTNNB1* mRNA contributes to CRC progression. Dashwood and co-workers were the first to compare the presence of several regulatory elements within the rat and human *CTNNB1* promoters, and specifically identified a ZBP-89 DNA binding site within the first 2000 bp of the rat promoter (9). By contrast, the human *CTNNB1* promoter is more GC-rich, contains a TATA box and 3 putative GC-rich Sp1 sites within the first 150 bp of

the transcriptional start site (10). However, the function of these proximal GC-rich elements was not functionally tested.

Zinc Finger Binding Protein-89 kDa (ZBP-89 protein encoded by the human *ZNF148* or mouse *Zfp148* locus) is a ubiquitously expressed *Krüppel*-type zinc finger transcription factor that binds GC-rich DNA elements frequently in concert with Sp1 (11-13). ZBP-89 is required for mucosal protection in the colon when challenged with a pathogen and mediates mucosal restitution mechanisms that work in concert with the Wnt- $\beta$ catenin pathway (14, 15). Furthermore, we found that mice carrying a conditional deletion of *Zfp148* in intestinal epithelial cells (*Zfp148*<sup>ΔIEC</sup>) are more susceptible to mucosal damage from infectious agents in part due to reduced tissue levels of serotonin and anti-microbial peptides (15, 16). ZBP-89 synergizes with  $\beta$ -catenin to induce mucosal defense genes encoding tryptophan hydroxylase1 and antimicrobial peptides called defensins (15). Having established that ZBP-89 and  $\beta$ -catenin functionally cooperate in the normal colon, we considered whether ZBP-89 regulates *CTNNB1* gene expression not only to restore homeostasis but also in promoting neoplastic transformation.

In a study of 742 CRCs, *ZNF148* gene expression increased in the transition from normal to stage 1 CRC but then decreased at later stages of cancer progression (Stages III and IV) (17). This study was consistent with a prior report indicating that *ZNF148* is down-regulated in colorectal cancers that progress to stage III (18). We previously showed that ZBP-89 forms a protein-protein complex with the tumor suppressor p53 (19) and recent reports indicate

that it suppresses p53 function since genetic deletion of one *Zfp148* allele increases p53 activity (20, 21). Moreover, other reports have shown that ZBP-89 protein expression promotes esophageal, renal cell and hepatocellular carcinoma (22-24). Since increased ZBP-89 mRNA and protein expression occurs in several cancers including stomach (25) and CRC(17), we hypothesized that the transcription factor likely plays an essential role in tumorigenesis and examined whether ZBP-89 synergizes with Wnt signaling through its ability to regulate *CTNNB1* gene expression.

## Materials and Methods

**Human Tissue Arrays.** Three human tissue arrays (COC1501, COC1502, COC1503) containing representative samples in duplicate 1.1 mm sections of human colon (4-normal colon tissue, 11-adenomas and colorectal cancers-193) were purchased from Pantomics (Richmond, CA; [www.pantomics.com](http://www.pantomics.com)) and include the age, gender, pathology, tumor grade and stage.

**Kaplan-Meier Survival Curves.** Survival curves were generated from Affymetrix microarray data deposited in the Gene Expression Omnibus (GEO, <http://www.ncbi.nlm.nih.gov/geo/>). The search terms were “colon”, “cancer”, “GPL96”, “GPL570”, “GPL571”, “survival” as well as any combination. Only the GEO files with survival data were used and are as follows: RFS total = 1373: GSE12945 n=51; GSE14333 n=226; GSE17538 n=232; GSE31595 n=37; GSE33114 n=90; GSE37892 n=130; GSE39582 n=519; GSE41258 n=115. Twenty-seven of the 1400 samples in the 8 datasets did not report the survival data and were therefore excluded from the analysis. Therefore only files with survival data were used. Gene expression and the “relapse-free survival” data were integrated simultaneously into one database. To analyze the prognostic value of the *ZNF148* probes *BERF-1* or *BFCOL*, the colon cancer patient samples were split into two groups according to high versus low levels of gene expression and then were used to generate Kaplan-Meier plots of “relapse-free survival”. To define a cut-off value, we computed a Cox regression analysis for each percentile between the lower and upper quartiles of gene expression and

the best threshold was used when drawing the Kaplan-Meier plot (26). The hazard ratios with 95% confidence intervals and log rank *P* value were calculated as described previously (27).

**Animal models.** Generation of *Zfp148*<sup>FL/FL</sup> mice on a C57BL/6 genetic background are previously described (15). *Apc*<sup>FL/+</sup>, *Zfp148*<sup>FL/+</sup> and *Zfp148*<sup>FL/FL</sup> mice were bred to the *VillinCre* (VC) line to generate mice that were heterozygous for the *Apc* allele alone or were expressed with the *Zfp148*<sup>FL/+</sup> and *Zfp148*<sup>FL/FL</sup> genotypes. All methods and procedures were approved by the University of Michigan Animal Care and Use Committee, which maintains an American Association of Assessment and Accreditation of Laboratory Animal Care facility.

**Plasmids and Cell Lines.** Upon receipt, frozen stocks were generated, checked for mycoplasma within 3 months of experiments and used between 3 and 20 passages after receipt. HEK293 and SW480 colon cell lines were purchased from ATCC in 2015, and the DLD-1 line in 2016. The KM12 cell lines were purchased from the NCI Repository in 2013. The DLD-1 and RKO cell lines were kindly provided by Eric Fearon (University of Michigan). All lines except DLD-1 and RKO were cultured in DMEM (GIBCO, Life Technologies) supplemented with 10% fetal bovine serum (FBS) and antibiotics (100 U/mL penicillin plus 100 µg/mL streptomycin). RKO and DLD-1 cells were cultured in RPMI 1640 with 10% FBS, glutamine and antibiotics.

**Transient Transfections.** WT and mutant (Mut) *CTNNB1*-Luc reporters (75 ng per well) with 2 ng /well of Renilla reporter were transfected with

Lipofectamine 2000 (Life Technologies) into SW480 cells cultured on 12-well plates 24h. Firefly luciferase was normalized to Renilla. Each experiment was performed in duplicate three times. siRNA transfections were carried out using Lipofectamine RNAi-MAX in antibiotic-free medium. siRNA oligos for *ZNF148* were a pooled mixture of 4 genomic sequences (siGENOME SMARTpool, Dharmacon #M-012658-01). Pooled *CTNNB1* siRNAs were from Fisher Scientific (#AM16708).

**Chromatin immunoprecipitation (ChIP).** SW480 cells were treated with 1% formaldehyde and then quenched with glycine for 5 min at room temperature. Cell lysates (500 $\mu$ l) were sonicated to shear DNA into primarily 200 to 1000 bp fragments (4 cycles of 30 sec intervals) using a 130W Sonics Vibracell (VCX130PB, Newton, CT). An aliquot (5%) was removed from the sonicate for total input DNA and the remainder (475 $\mu$ l) was used to immunoprecipitate crosslinked protein with either ZBP-89 antibody or IgG (antibody control). Immune complexes were captured using Protein A/G agarose beads. After repeated washes the bound proteins were eluted from the beads and diluted 1:15 in deionized water (EZ Magna ChIP A/G Kit, #17-10086, Millipore, MA). After proteinase K and RNAase A digestions, precipitated chromatin fragments were analyzed by PCR using Nova*Taq* DNA Polymerase, (Millipore) and 3 sets of primers flanking the *CTNNB1*, *ZNF148* or *ChrA* promoter regions (Supplemental data).

To perform ChIP analysis of  $\beta$ -catenin binding to the *ZNF148* promoter, the transcriptional start site was identified *in silico* using transcript alignment and



the site of POL2A binding within the UCSC Genome browser (<http://genome.ucsc.edu>). ChIP-qPCR values expressed as a percent of input DNA after sequence confirmation. Primers for human chromogranin A (ChgA) were used as the non-related promoter control. PCR products were resolved on a 1% agarose gel, sequenced and then quantified by qPCR for triplicate experiments.

**Quantitative Real-Time PCR.** Cultured cells were harvested in Trizol (Invitrogen) for RNA extraction and DNase-treatment. Quantitative PCR analysis was carried out on triplicate cDNA samples using the BIO-RAD C1000 thermal cycler, analyzed with CFX ManagerV2 software and normalized to *Hprt*.

Experiments were performed at least three times in triplicate. Mouse PCR primer pairs for *Zfp148* were:

forward: 5'-GGC ATG TCT TCA TTC ATA GAG G;  
reverse: 5'-CTC ATA CCA CAT TCA TCA CAG C

*Hprt* primer pairs were:

forward: 5'-AGT CCC AGC GTC GTG ATT AGC;  
reverse: 5'-ATA GCC CCC CTT GAG CAC ACA G.

**Colony Formation Assay.** DLD-1 and RKO cells were seeded onto 6-well plates in growth medium (10% FBS) at 1000 cells/well. For KM12 L4 and SW480 cells, 100 cells/well were seeded onto 6-well plates in growth media containing 10% FBS. Sixteen hours after plating, the cells were transfected with 25 nM siGenome SMARTpool siRNAs for *ZNF148* (M-012658-01, Dharmacon, Chicago, IL), *CTNNB1* (M-003482-00, Dharmacon) or non-targeted controls (Con) (D-001206-13, Dharmacon). Media was replenished every three days with

siRNAs or non-targeted controls until colonies formed at week 3. Plating efficiency was 20%. The wells were rinsed with PBS, fixed in 10% formalin for 30 minutes, and then stained for counting with a solution of 0.1% crystal violet. The number of colonies formed for each treatment was expressed as a percentage of the non-targeted control siRNA.

**MTT Assay.** The MTT assay was performed according to manufacturer's instructions. Briefly, RKO, DLD-1, KM-12 and SW480 cells (1000 cells per well), were transfected with the gene specific and non-targeted siRNA oligos (25 nM). Four days after transfection, 0.5 mg/mL of MTT labeling solution was added to each well and incubated for 4 hours at 37°C. Formazan crystals generated were dissolved by incubating with the solubilization reagent overnight, and the absorbance was measured on plate reader at  $A_{570}$  and reference wavelength of  $A_{660}$ . Cell viability was determined using the equation  $A_{570} - A_{660}$  (cells transfected with *CTNNB1* or *ZNF148* siRNA) /  $\{A_{570} - A_{660}$  (cells transfected with control siRNA)  $\} \times 100$ . The indicated cell lines were plated in 96-well (1000 cells per well) plates. Twenty-four hours after plating, the cells were transfected with 25nM of a non-targeted, *ZNF148* or *CTNNB1* siRNA using PolyJet transfection reagent (SIGNAGen) according to the manufacturer's instructions. The S33Y cDNA expression vector was transfected 24h after transfection of the siRNA again using the PolyJet reagent. Two days after both transfections, 0.5 mg/ml of MTT labeling solution was added, incubated for 4h at 37°C and then measured as described above.

**Intestinal Enteroid Generation.** The intestinal mucosa was minced into 5 mm pieces on ice followed by gland dissociation in 2mM EDTA/PBS at 4°C for 30min. After filtration through a 100µm nylon mesh, the suspension was centrifuged at 200×g for 5min, the glands were re-suspended in 50µl of Matrigel supplemented with Advanced DMEM/F12, (Invitrogen) containing 50% Wnt plus R-Spondin conditioned media generated from stably-expressing L cells (28) with additional factors purchased from Invitrogen, i.e., Noggin (100ng/ml) and EGF (50ng/ml), and then cultured at 37°C in 5% CO<sub>2</sub>. Two days after culturing the crypt-Matrigel, suspension enteroids were observed in the WT crypt cultures. The presence of budding enteroids versus spheroids was enumerated over 8 days after the initial plating plus 3 additional passages.

**Statistical Analysis.** Comparison among multiple histologic groups was performed using Kruskal-Wallis as detailed above. One-way ANOVA with Tukey's test for multiple comparisons was used to compare polyp numbers, normalized luciferase values, MTT and colony forming assays. Two-way ANOVA was used to analyze the enteroid/spheroid time course.

## Results

### Increased *ZNF148* expression correlates with poor survival in CRC

Although elevated ZBP-89 protein expression correlates with poor survival in colorectal and esophageal adenocarcinomas (17, 18, 22), The Cancer Genome Atlas (TCGA) databases show that the *ZNF148* locus that encodes ZBP-89 is mutated in only 1.4% of CRCs (total of 504 cases from 3 databases) (Table S1). To examine ZBP-89 protein expression in the colon at different histological stages, immunohistochemical analysis was performed on 3 sets of colorectal cancer (CRC) tissue arrays. ZBP-89 protein expression in normal human colon was low as observed for  $\beta$ -catenin protein expression (Fig. 1A, B). Although most of the ZBP-89 staining remained cytoplasmic and/or membranous (Figs. 1C, E, G, I, K) and was completely negative in 2.6% of the samples, the intensity of ZBP-89 expression in adenomas increased significantly in parallel with increased  $\beta$ -catenin expression compared to normal colon (Fig. 1C, D). Moreover, the membranous and cytoplasmic staining pattern for both ZBP-89 and  $\beta$ -catenin in CRC was consistent with prior reports (<http://www.proteinatlas.org>). Nuclear  $\beta$ -catenin was initially observed in stage 1 and stage 2 CRCs and coincided with ~60% of the tissues expressing ZBP-89 protein (Fig. 1E-L). The intensity of the signal for both proteins remained elevated in all four cancer stages compared to normal colon (Fig. 1M, N). In addition, we examined whether elevated *ZNF148* mRNA expression correlated with survival. Microarray datasets for colorectal cancer were downloaded from the Gene Omnibus Expression (GEO) public database for analysis using two probe sets

(*BFCOL* and *BERF1*) that recognize sequences at the C-terminus and 3'UTR of *ZNF148* (Fig. S1). Elevated *ZNF148* mRNA expression levels in CRC patients correlated with worse relapse-free survival compared to patients with low levels of expression (Fig. 1O,P). Therefore we tested the hypothesis that elevated ZBP-89 expression contributes to adenoma progression to cancer after disruption of one *Apc* allele, which generates higher levels of  $\beta$ -catenin due to protein stabilization.

### **Conditional *Zfp148* deletion reduced *Apc*<sup>+/ $\Delta$ IEC</sup>-mediated polyp formation**

To determine how ZBP-89 expression contributes to adenoma progression, we conditionally-deleted one or both *Zfp148* alleles in a mouse model of  $\beta$ -catenin-driven polyps in which one *Apc* allele was also conditionally-deleted using the *VillinCre* mouse line (*VC:Apc*<sup>+/*FL*</sup>;*Zfp148*<sup>*FL/FL*</sup>, hereafter referred to as *Apc*<sup>+/ $\Delta$ IEC</sup>;*Zfp148* <sup>$\Delta$ IEC</sup>). Deletion of one or both *Zfp148* alleles alone does not alter intestinal growth (15), consistent with no significant difference in Ki67 staining in the crypt zone (Fig. S2). Therefore the *Zfp148* <sup>$\Delta$ IEC</sup> mice were placed on the mutant *Apc* genetic background (*Apc*<sup>+/ $\Delta$ IEC</sup>), to stabilize the cellular levels of  $\beta$ -catenin, and subsequently predispose the intestinal mucosa to hyperplasia and polyp formation. Deletion of one or both *Zfp148* alleles significantly reduced  $\beta$ -catenin protein and mRNA tissue levels (Fig. 2A,B). Mice heterozygous for the *Apc* allele (*Apc*<sup>+/ $\Delta$ IEC</sup>) generated numerous small intestinal polyps within 5 months after birth (Fig. 2C-E), consistent with prior reports (29). Moreover, deleting one or both *Zfp148* alleles significantly reduced the number of intestinal polyps (Fig. F), but not the size or location of the *Apc*-dependent polyps (Fig. 2H, I).

Insufficient numbers of polyps developed in the colon to assess the effect of deleting *Zfp148* (Fig. 2G). In the context of the *Apc* deletion alone,  $\beta$ -catenin protein levels were higher than with intact *Apc* loci, and there was no significant effect on mRNA levels (Fig. 2A,B versus 2D,E). Elevated levels of  $\beta$ -catenin protein persisted even with the loss of one or both *Zfp148* alleles (Fig. 2D) due to stabilization of  $\beta$ -catenin protein with deletion of one *Apc* allele (30, 31). Nevertheless deleting both *Zfp148* alleles significantly decreased both  $\beta$ -catenin protein and mRNA (Fig. 2D,E). Collectively, these results were consistent with direct transcriptional induction of the *ctnnb1* promoter by ZBP-89 or indirectly through mRNA stability contributing to the cellular pool of  $\beta$ -catenin protein.

### ***ZNF148* deletion reduces Wnt-dependent cell growth**

To further test the functional dependence of  $\beta$ -catenin expression on ZBP-89, colony-forming assays were performed after knocking down *ZNF148* expression by siRNA in  $\beta$ -catenin-dependent CRC cell lines (DLD-1, SW480), which produces truncated APC protein (32) or  $\beta$ -catenin -independent CRC cell lines (RKO, KM12), which produce wild type APC (33) (Fig. 3A,B). Reduced ZBP-89 expression decreased colony formation (Fig. 3A,B) and cell viability (Fig. 3C) in the  $\beta$ -catenin-dependent cell lines by 50% but had no effect on the  $\beta$ -catenin -independent cell lines. Reducing ZBP-89 expression decreased  $\beta$ -catenin protein expression; while siRNA-mediated knockdown of *CTNNB1* also reduced ZBP-89 expression (Fig. 3D).

Reducing *CTNNB1* expression depressed colony formation by ~90% in the  $\beta$ -catenin-dependent, but not the  $\beta$ -catenin-independent cell lines (Fig. 3A-D).

Furthermore, reduced cell viability in the SW480 line was reversed by over-expressing constitutively active S33Y mutant  $\beta$ -catenin protein, but had no effect on the viability of the  $\beta$ -catenin-independent KM12 cell line (Fig. S3). Thus we concluded that ZBP-89 modulation of cell growth in a Wnt-dependent cell line requires  $\beta$ -catenin. In addition, increasing ZBP-89 expression dose-dependently increased  $\beta$ -catenin protein as well as colony growth in the DLD-1 cell line (Fig. 3E,F). Therefore in the context of Wnt signaling, ZBP-89 was necessary and sufficient for Wnt-dependent cell growth.

### **Zfp148 deletion promotes enteroid budding**

Wnt signaling is highest at the base of the intestinal crypt where the stem cells reside (34). Formation and sustained propagation of intestinal enteroids requires cells from the stem cell niche (35). Deletion of *Apc* accompanied by elevated Wnt signaling promotes spheroid-shaped enteroids remarkable for the absence of crypt buds (35). As previously reported (36), we found that enteroids from wild type mice form budding appendages indicative of cells from the intestinal crypt comprised of a mixture of stem and transit-amplifying cells (Fig. 4A). By contrast, glands isolated from *Apc* <sup>$\Delta$ IEC/+</sup> mice remain spheroid consistent with high Wnt activity and maintenance of the stem cell phenotype (Fig. 4B) and were readily quantified (Fig. 4C). Enteroids prepared from the *Zfp148* <sup>$\Delta$ IEC/ $\Delta$ IEC</sup> mice did not exhibit significant differences in their ability to form budding enteroids compared to the Cre negative control enteroids (Fig. 4D, E). By contrast, glands from *Apc* <sup>$\Delta$ IEC/+</sup>; *Zfp148* <sup>$\Delta$ IEC/+</sup> mice over time exhibited some budding compared to the *Apc* <sup>$\Delta$ IEC/+</sup> enteroids, which generated small enteroids

by day 8 (Fig. 4D, E). Therefore the spheroid phenotype correlated with synergy between *Zfp148* and elevated Wnt signaling in the stem cell niche after loss of one *Apc* allele; while budding occurred with deletion of one *Zfp148* allele. Enteroids did not develop after deletion of both *Zfp148* alleles even in the absence of one *Apc* allele (*Apc* <sup>$\Delta$ IEC/+</sup>), indicating a requirement for *Zfp148* expression to form enteroids. Apparently elevated Wnt signaling in the absence of even one *Zfp148* allele was sufficient to induce budding.

### **ZBP-89 directly regulates the *CTNNB1* promoter**

Hypothesizing that ZBP-89 directly binds to the *CTNNB1* promoter, we identified a consensus ZBP-89 site at -120 bp *in silico* upstream from the transcriptional start site of the human *CTNNB1* gene (Fig. 5A). ChIP analysis revealed that the most proximal *ZNF148* element at -120 bp (within the -209 to -1 segment) contained the highest affinity DNA binding site compared to overlapping DNA segments at -422 to -261 and -539 to -391 (Fig. 5A). The putative GC-rich ZBP-89 binding site at -120 was examined further by EMSA and revealed several complexes. A portion of the upper complex contained Sp1 since the addition of Sp1 antibody super-shifted the complex. There was decreased probe binding when ZBP-89 antibody was added, indicating that a component of the same complex contained ZBP-89 (Fig. 5B). We used DNA affinity precipitation (DAPA) using a biotinylated probe to further demonstrate that ZBP-89 binds specifically to the DNA element at -120 bp (Fig. 5C). Adding WT oligo competitively eliminated protein binding to the biotinylated probe (Fig. 5B, lane 3) while protein binding was retained with the addition of the 2-bp mutant oligo (Fig.



5B, lane 4). Next, we showed that full-length ZBP-89 expression induced a *CTNNB1* luciferase reporter containing 591 bp of the promoter but did not induce the reporter in both SW480 and HEK293 cells if the 2-bp point mutation was introduced into the ZBP-89 DNA binding site at -120 (Fig. 5D,E,G). Co-transfecting ZBP-89 deletion mutants with the reporter plasmid revealed that induction required the presence of zinc fingers located within the amino terminal domain (Fig. 5D,F,H). Therefore ZBP-89 protein binds directly to the *CTNNB1* promoter to induce transcription. This mechanism was also consistent with the observation that removal of the *Zfp148* alleles decreased  $\beta$ -catenin mRNA and protein expression in the intestinal glands, which subsequently decreased polyp formation in *Apc* mutant mice (see Fig. 2).

Since the knockdown of *CTNNB1* expression decreased ZBP-89 expression (Fig. 3C), we tested the possibility that Wnt- $\beta$ -catenin signaling induces the *ZNF148* locus subsequently increasing the cellular levels of ZBP-89 protein. *In silico* analysis of the proximal *ZNF148* promoter revealed putative TCF/LEF sites between -987 and -583 (Genomatix), which was confirmed by ChIP analysis using antibodies to  $\beta$ -catenin (Fig. 6A-C). Ectopic expression of WT or constitutively active  $\beta$ -catenin in SW480 cells induced *ZNF148* mRNA most dramatically in the presence of Wnt3A conditioned media (Fig. 6D). Furthermore, ectopic expression of ZBP-89 slightly induced *ZNF148* mRNA expression, suggesting some degree of self-regulation (Fig. 6D). Thus, since both ZBP-89 and  $\beta$ -catenin reciprocally induced gene expression of each other,

the results collectively suggested feedforward synergy between the *CTNNB1* and *ZNF148* loci (Fig. 7).

## **Discussion**

Mutations in the *APC* gene locus increase cellular levels of  $\beta$ -catenin through a variety of pathways (2). However, the primary focus has generally been on post-translational mechanisms resulting in  $\beta$ -catenin protein stabilization and its translocation to the nucleus after dissociation from wild type APC protein,  $\beta$ -catenin phosphorylation, ubiquitinylation and shuttling to the proteasome. More recently, reports have acknowledged that *CTNNB1* gene expression also contributes to increased cellular levels of this proto-oncogene in the context of *APC* mutations and appears to be related especially to the degree of CRC invasiveness (8). Yet the transcription factors inducing its gene expression have not been examined in detail. Comparative analysis of the *CTNNB1* promoter among mammalian species indicates that it is GC-rich and contains several putative Sp1/ZBP-89 binding sites within the proximal promoter(10).

The ZBP-89 transcription factor family consists of 2 other genes—*ZNF281* and *ZNF740* (genecards.org). *ZNF281* encodes ZBP-99 protein, which recognizes the same GC-rich binding site as ZBP-89 since their DNA binding domains are 79% identical and 91% similar (37). We therefore considered that ZBP-99 and ZBP-89 might regulate some of the same target genes. Coincidentally, the role of ZBP-99 in intestinal stem cells has been studied in some detail with respect to regulating  $\beta$ -catenin and CRC cancer progression (38, 39). Specifically, the transcription factor SNAIL, which promotes epithelial to

mesenchymal transition (EMT) directly induces *ZNF281* gene expression. Moreover, quantitative ChIP analysis revealed that ZBP-99 occupies the promoter of the Wnt target gene *LGR5*, which ultimately increases  $\beta$ -catenin activity and the acquisition of stem cell traits (38). ZBP-99 binds the proximal *CTNNB1* promoter and induces *CTNNB1* mRNA in osteogenic stem cells, demonstrating that a ZBP-89 family member directly binds and regulates *CTNNB1* gene expression (40). Thus, ZBP-99, a ZBP-89 family member, is able to indirectly regulate  $\beta$ -catenin activity in CRC cell lines, and directly bind to the *CTNNB1* promoter in specific cell types, suggesting that ZBP-89 might also regulate *CTNNB1* gene expression.

Like ZBP-99, we show here that ZBP-89 also directly binds the *CTNNB1* promoter. ZBP-89 binding contributed to elevated  $\beta$ -catenin activity since deleting one or both *Zfp148* alleles was sufficient to reduce  $\beta$ -catenin mRNA and protein expression, resulting in fewer polyps. Moreover, elevated  $\beta$ -catenin activity in *Apc* mutant organoids lost its stem cell phenotype (spheroid shape), when *Zfp148* was deleted, suggesting that ZBP-89 also correlates with stemness. A recent report of *Zfp148* deficiency also found reduced polyp formation in an *Apc<sup>min</sup>* model of intestinal polyps but did not detect changes in  $\beta$ -catenin (21), perhaps due to reduced *Zfp148* in the immune compartment where ZBP-89 is also highly expressed (12).

At least 80 percent of CRCs exhibit *APC* mutations and correspond to elevated levels of  $\beta$ -catenin protein raising the question as to how *ZNF148* gene expression increases under conditions of elevated  $\beta$ -catenin levels (31). Indeed

we found that knocking down *CTNNB1* mRNA was sufficient to dramatically reduce ZBP-89 protein expression. Thus, we conclude that  $\beta$ -catenin protein accumulates in the absence of a functional *APC* allele and initiates a program of cell proliferation through its target genes, including induction of *ZNF148* gene expression. Subsequently, sustained levels of *CTNNB1* expression can be maintained through the binding of ZBP-89 protein to the *CTNNB1* promoter further expanding the pool of  $\beta$ -catenin protein. The absence of *ZNF148* mutations yet increased mRNA levels in *APC*<sup>+/-</sup>-dependent tumors suggest that unregulated Wnt signaling initiates the increase in ZBP-89 gene expression. In this way, the two transcriptional regulators provide a “feedforward” mechanism to sustain unregulated  $\beta$ -catenin signaling in the stem cell niche (Fig. 7).

## References

1. Schneikert, J., and Behrens, J. The canonical Wnt signalling pathway and its APC partner in colon cancer development. *Gut* 2007. 56:417-425.
2. Polakis, P. Wnt signaling and cancer. *Genes Dev* 2000. 14:1837-1851.
3. Herbst, A., Jurinovic, V., Krebs, S., Thieme, S.E., Blum, H., Goke, B., and Kolligs, F.T. Comprehensive analysis of beta-catenin target genes in colorectal carcinoma cell lines with deregulated Wnt/beta-catenin signaling. *BMC Genomics* 2014. 15:74.
4. Moon, R.T., Bowerman, B., Boutros, M., and Perrimon, N. The promise and perils of Wnt signaling through beta-catenin. *Science* 2002. 296:1644-1646.
5. El-Bahrawy, M.A., Poulsom, R., Jeffery, R., Talbot, I., and Alison, M.R. The expression of E-cadherin and catenins in sporadic colorectal carcinoma. *Hum Pathol* 2001. 32:1216-1224.
6. Mann, B., Gelos, M., Siedow, A., Hanski, M.L., Gratchev, A., Ilyas, M., Bodmer, W.F., Moyer, M.P., Riecken, E.O., Buhr, H.J., et al. Target genes of beta-catenin-T cell-factor/lymphoid-enhancer-factor signaling in human colorectal carcinomas. *Proc Natl Acad Sci U S A* 1999. 96:1603-1608.
7. Guigon, C.J., Kim, D.W., Zhu, X., Zhao, L., and Cheng, S.Y. Tumor suppressor action of liganded thyroid hormone receptor beta by direct repression of beta-catenin gene expression. *Endocrinology* 2010. 151:5528-5536.
8. Bandapalli, O.R., Dihlmann, S., Helwa, R., Macher-Goeppinger, S., Weitz, J., Schirmacher, P., and Brand, K. Transcriptional activation of the beta-catenin gene at the invasion front of colorectal liver metastases. *J Pathol* 2009. 218:370-379.
9. Li, Q., Dashwood, W.M., Zhong, X., Al-Fageeh, M., and Dashwood, R.H. Cloning of the rat beta-catenin gene (Ctnnb1) promoter and its functional analysis compared with the Catnb and CTNNB1 promoters. *Genomics* 2004. 83:231-242.
10. Nollet, F., Berx, G., Molemans, F., and van Roy, F. Genomic organization of the human beta-catenin gene (CTNNB1). *Genomics* 1996. 32:413-424.
11. Merchant, J.L., Iyer, G.R., Taylor, B.R., Kitchen, J.R., Mortensen, E.R., Wang, Z., Flintoft, R.J., Michel, J.B., and Bassel-Duby, R. ZBP-89, a Kruppel-like zinc finger protein, inhibits epidermal growth factor induction of the gastrin promoter. *Mol Cell Biol* 1996. 16:6644-6653.

12. Law, G.L., Itoh, H., Law, D.J., Mize, G.J., Merchant, J.L., and Morris, D.R. Transcription factor ZBP-89 regulates the activity of the ornithine decarboxylase promoter. *J Biol Chem* 1998. 273:19955-19964.
13. Bai, L., and Merchant, J.L. Transcription factor ZBP-89 cooperates with histone acetyltransferase p300 during butyrate activation of p21waf1 transcription in human cells. *J Biol Chem* 2000. 275:30725-30733.
14. Law, D.J., Labut, E.M., Adams, R.D., and Merchant, J.L. An isoform of ZBP-89 predisposes the colon to colitis. *Nucleic Acids Res* 2006. 34:1342-1350.
15. Essien, B.E., Grasberger, H., Romain, R.D., Law, D.J., Veniaminova, N.A., Saqui-Salces, M., El-Zaatari, M., Tessier, A., Hayes, M.M., Yang, A.C., et al. ZBP-89 Regulates Expression of Tryptophan Hydroxylase I and Mucosal Defense Against Salmonella Typhimurium in Mice. *Gastroenterology* 2013. 144:1466-1477.
16. Kemmerly, T., and Kaunitz, J.D. Gastroduodenal mucosal defense. *Curr Opin Gastroenterol* 2014. 30:583-588.
17. Gao, X.H., Liu, Q.Z., Chang, W., Xu, X.D., Du, Y., Han, Y., Liu, Y., Yu, Z.Q., Zuo, Z.G., Xing, J.J., et al. Expression of ZNF148 in different developing stages of colorectal cancer and its prognostic value: a large Chinese study based on tissue microarray. *Cancer* 2013. 119:2212-2222.
18. Bandres, E., Malumbres, R., Cubedo, E., Honorato, B., Zarate, R., Labarga, A., Gabisu, U., Sola, J.J., and Garcia-Foncillas, J. A gene signature of 8 genes could identify the risk of recurrence and progression in Dukes' B colon cancer patients. *Oncol Rep* 2007. 17:1089-1094.
19. Bai, L., and Merchant, J.L. ZBP-89 promotes growth arrest through stabilization of p53. *Mol Cell Biol* 2001. 21:4670-4683.
20. Sayin, V.I., Khan, O.M., Pehlivanoglu, L.E., Staffas, A., Ibrahim, M.X., Asplund, A., Agren, P., Nilton, A., Bergstrom, G., Bergo, M.O., et al. Loss of one copy of Zfp148 reduces lesional macrophage proliferation and atherosclerosis in mice by activating p53. *Circ Res* 2014. 115:781-789.
21. Nilton, A., Sayin, V.I., Zou, Z.V., Sayin, S.I., Bondjers, C., Gul, N., Agren, P., Fogelstrand, P., Nilsson, O., Bergo, M.O., et al. Targeting Zfp148 activates p53 and reduces tumor initiation in the gut. *Oncotarget* 2016.
22. Yan, S.M., Wu, H.N., He, F., Hu, X.P., Zhang, Z.Y., Huang, M.Y., Wu, X., Huang, C.Y., and Li, Y. High expression of zinc-binding protein-89 predicts decreased survival in esophageal squamous cell cancer. *Ann Thorac Surg* 2014. 97:1966-1973.

23. Cai, M.Y., Luo, R.Z., Li, Y.H., Dong, P., Zhang, Z.L., Zhou, F.J., Chen, J.W., Yun, J.P., Zhang, C.Z., and Cao, Y. High-expression of ZBP-89 correlates with distal metastasis and poor prognosis of patients in clear cell renal cell carcinoma. *Biochem Biophys Res Commun* 2012. 426:636-642.
24. Zhang, C.Z., Cao, Y., Yun, J.P., Chen, G.G., and Lai, P.B. Increased expression of ZBP-89 and its prognostic significance in hepatocellular carcinoma. *Histopathology* 2012. 60:1114-1124.
25. Taniuchi, T., Mortensen, E.R., Ferguson, A., Greenson, J., and Merchant, J.L. Overexpression of ZBP-89, a zinc finger DNA binding protein, in gastric cancer. *Biochem Biophys Res Commun* 1997. 233:154-160.
26. Mihaly, Z., Kormos, M., Lanczky, A., Dank, M., Budczies, J., Szasz, M.A., and Gyorffy, B. A meta-analysis of gene expression-based biomarkers predicting outcome after tamoxifen treatment in breast cancer. *Breast Cancer Res Treat* 2013. 140:219-232.
27. Gyorffy, B., Surowiak, P., Budczies, J., and Lanczky, A. Online survival analysis software to assess the prognostic value of biomarkers using transcriptomic data in non-small-cell lung cancer. *PLoS One* 2013. 8:e82241.
28. Miyoshi, H., Ajima, R., Luo, C.T., Yamaguchi, T.P., and Stappenbeck, T.S. Wnt5a potentiates TGF-beta signaling to promote colonic crypt regeneration after tissue injury. *Science* 2012. 338:108-113.
29. Hinoi, T., Akyol, A., Theisen, B.K., Ferguson, D.O., Greenson, J.K., Williams, B.O., Cho, K.R., and Fearon, E.R. Mouse model of colonic adenoma-carcinoma progression based on somatic Apc inactivation. *Cancer Res* 2007. 67:9721-9730.
30. Rosenbluh, J., Wang, X., and Hahn, W.C. Genomic insights into WNT/beta-catenin signaling. *Trends Pharmacol Sci* 2014. 35:103-109.
31. White, B.D., Chien, A.J., and Dawson, D.W. Dysregulation of Wnt/beta-catenin signaling in gastrointestinal cancers. *Gastroenterology* 2012. 142:219-232.
32. Yang, J., Zhang, W., Evans, P.M., Chen, X., He, X., and Liu, C. Adenomatous polyposis coli (APC) differentially regulates beta-catenin phosphorylation and ubiquitination in colon cancer cells. *J Biol Chem* 2006. 281:17751-17757.
33. Dang, D.T., Mahatan, C.S., Dang, L.H., Agboola, I.A., and Yang, V.W. Expression of the gut-enriched Kruppel-like factor (Kruppel-like factor 4)

- gene in the human colon cancer cell line RKO is dependent on CDX2. *Oncogene* 2001. 20:4884-4890.
34. van de Wetering, M., Sancho, E., Verweij, C., de Lau, W., Oving, I., Hurlstone, A., van der Horn, K., Batlle, E., Coudreuse, D., Haramis, A.P., et al. The beta-catenin/TCF-4 complex imposes a crypt progenitor phenotype on colorectal cancer cells. *Cell* 2002. 111:241-250.
  35. Dow, L.E., O'Rourke, K.P., Simon, J., Tschaharganeh, D.F., van Es, J.H., Clevers, H., and Lowe, S.W. Apc Restoration Promotes Cellular Differentiation and Reestablishes Crypt Homeostasis in Colorectal Cancer. *Cell* 2015. 161:1539-1552.
  36. Sato, T., Vries, R.G., Snippert, H.J., van de Wetering, M., Barker, N., Stange, D.E., van Es, J.H., Abo, A., Kujala, P., Peters, P.J., et al. Single Lgr5 stem cells build crypt-villus structures in vitro without a mesenchymal niche. *Nature* 2009. 459:262-265.
  37. Law, D.J., Du, M., Law, G.L., and Merchant, J.L. ZBP-99 defines a conserved family of transcription factors and regulates ornithine decarboxylase gene expression. *Biochem Biophys Res Commun* 1999. 262:113-120.
  38. Hahn, S., Jackstadt, R., Siemens, H., Hunten, S., and Hermeking, H. SNAIL and miR-34a feed-forward regulation of ZNF281/ZBP99 promotes epithelial-mesenchymal transition. *EMBO J* 2013. 32:3079-3095.
  39. Hahn, S., and Hermeking, H. ZNF281/ZBP-99: a new player in epithelial-mesenchymal transition, stemness, and cancer. *J Mol Med (Berl)* 2014. 92:571-581.
  40. Seo, K.W., Roh, K.H., Bhandari, D.R., Park, S.B., Lee, S.K., and Kang, K.S. ZNF281 knockdown induced osteogenic differentiation of human multipotent stem cells in vivo and in vitro. *Cell Transplant* 2013. 22:29-40.



**Acknowledgements**

The authors thank the Molecular Biology Core of the UM DDRC P30 DK-034933 and Frederick L. McDonald III for assisting with primer development for the *ZNF148* promoter and schematic figure design.

## Figure Legends

**Figure 1. Increased ZBP-89 protein expression in CRC correlates with reduced survival.** Representative images for ZBP-89 and  $\beta$ -catenin immunohistochemistry respectively using serial sections of tissue microarrays from normal human colon (A, B); adenoma (C, D); Adenocarcinoma, Stage 1 (E, F); Stage 2 (G, H); Stage 3 (I, J); Stage 4 (K, L). Magnification: 100 $\times$  and 400 $\times$  for the insets. The weighted scores of the immunohistochemical staining for ZBP-89 (M) or  $\beta$ -catenin (N) plotted as a function of the histology. P values for comparing the six groups were determined by Kruskal-Wallis. Curves of “survival-free relapse” for CRC patients over 200 months (16.6 years) for Affymetrix *ZNF148* probes designated *BFCOL1* and *BERF-1* (O, P). H.R. = Hazard ratio.

**Figure 2. Conditional deletion of *Zfp148* locus reduces intestinal polyp numbers in VC:*Apc*<sup>+/*FL*</sup> mice.** (A) Western blot and (B) mRNA levels for ZBP-89 and  $\beta$ -Catenin prepared from the intestinal mucosa of individual mice with the indicated genotypes *Zfp148*<sup>+/+</sup> (WT) (lanes 1,2); VC:*Zfp148*<sup>FL/+</sup> (lanes 3,4); VC:*Zfp148*<sup>FL/FL</sup> (lanes 5, 6) at age 4 to 5 months. GAPDH used as the loading control. Quantitative PCR for *Zfp148* (ZBP-89) or *ctnnb1* ( $\beta$ -catenin) mRNA normalized to *Hprt* mRNA. Shown is the mean  $\pm$ SEM for N= 5 experiments in performed in triplicate. \*\*P<0.01, NS= not significant for two transcripts within a genotype, one-way ANOVA with Tukey’s. An *Apc* allele was deleted in the intestinal epithelium by breeding the *Apc*<sup>+/*FL*</sup> mouse line to the VillinCre (VC) line

without (*Zfp148*<sup>+/+</sup>) or with deletion of one (*Zfp148*<sup>+/*FL*</sup>) or both *Zfp148* (*Zfp148*<sup>*FL/FL*</sup>) alleles. (C) Scanned slide of Swiss roll H&Es (1x) from *VC:Apc*<sup>+/*FL*</sup>; *VC:Apc*<sup>+/*FL*</sup>:*Zfp148*<sup>+/*FL*</sup>; *VC:Apc*<sup>+/*FL*</sup>:*Zfp148*<sup>*FL/FL*</sup> mice. Insets = 20x. (D) Western blot for ZBP-89 and  $\beta$ -catenin protein for individual mice with the indicated genotypes and (E) mRNA levels for *Zfp148* (ZBP-89) and *ctnnb1* ( $\beta$ -catenin) mRNA normalized to *Hprt*. Shown is the mean  $\pm$ SEM for N= 5 experiments performed in triplicate. \*P<0.003, \*\*\*P<0.0001. One-way ANOVA with Tukey's. Scatter graph of the number of polyps per mouse for the indicated genotypes in the intestine (F) and colon (G). Shown are the means  $\pm$ SD. \*P<0.02 or \*\*\*P<0.001, NS = not significant, one-way ANOVA with Tukey's. (H) Distribution of polyp location (percent of total number of polyps) per genotype; (I) Distribution of polyp size (percent of total number of polyps) per genotype. N = 7 mice per genotype.

**Figure 3.  $\beta$ -catenin-dependent cell growth requires ZBP-89. (A)**

Photomicrographs of crystal violet stained colonies from DLD-1, RKO, SW480 and KM12 cell lines 3 weeks after transfecting scrambled (siCont) or siRNA oligos for *ZNF148* (si<sup>*ZNF148*</sup>) and *CTNNB1* (si<sup>*CTNNB1*</sup>). (B) Number of colonies counted per plate (as a percent of the scrambled non-targeted control siCont) for each cell type. Shown is the mean  $\pm$ S.D. for N= 3 experiments performed in triplicate. \*P<0.02, \*\*P<0.002 and \*\*\*\*P<0.0001. No significant difference in the percentage of RKO and KM12 colonies among the 3 treatment groups. (C) MTT assay of cell viability for each of the 4 cell lines after 4 days. Shown is the mean

±S.D. as a percentage of the scrambled (SCR) control, \*\*P<0.002, \*\*\*P<0.002, \*\*\*\*P<0.0001, one-way ANOVA with Tukey's test. (D) Western blot of ZBP-89 and β-catenin protein expression normalized to GAPDH after transfection of siRNA oligos. (E) Western blot of ZBP-89 and β-catenin protein expression normalized to GAPDH after transfection of increasing amounts of *ZNF148* expression vector in pcDNA. (F) Number of colonies per plate graphed as a function of increasing amounts of *ZNF148* expression vector transfected compared to the pcDNA empty vector (0 ng). Shown is the mean ±S.D. for N = 3 experiments, \*\*\*P<0.001 compared to empty vector using one-way ANOVA. Representative photomicrographs of the crystal violet stained plates shown below for each amount of *ZNF148* expression vector transfected.

**Figure 4. Deletion of *Zfp148* induces budding of VC:*Apc*<sup>+/*FL*</sup> spheroids.**

Phase contrast micrographs of enteroid morphology from 1 to 8 days after plating dissociated glands from (A) WT (enteroid morphology) and (B) VC:*Apc*<sup>+/*FL*</sup> (*Apc*<sup>+/*ΔIEC*</sup>) mice (spheroid morphology). (C) Graph shows the percentage of enteroid (black) versus spheroids (grey) within the culture per day averaged from 3 passages per genotype. (D) Phase contrast micrographs of enteroid cultures per genotype (Cre negative-WT, *Zfp148*<sup>ΔIEC</sup>, *Apc*<sup>+/*ΔIEC*</sup> and *Apc*<sup>+/*ΔIEC*</sup>.*Zfp148*<sup>+/*ΔIEC*</sup>) at 1, 3 and 8 days after plating dissociated glands. (E) Graph shows the mean percentage of enteroid morphology per total structures (enteroids + spheroids) at day 3 and day 8 for 3 passages cultured in triplicate from 3 mice per genotype. Shown are the means ±SEM, \*\*P<0.001, \*\*\*P<0.0001 by two-way ANOVA.

**Figure 5. ZBP-89 binds to the *CTNNB1* promoter.** (A) Schematic of the human *CTNNB1* promoter. PCR primers were used to amplify 3 regions of the promoter (designated 1,2,3) between -539 and -1 bp upstream from the transcriptional start site following CHIP with ZBP-89 antibody. PCR products were analyzed on a 1% agarose gel and by qPCR as a percent of the input. \*\*\*P<0.001, one-way ANOVA with Tukey's. ChromograninA (CHRA) was used as an unrelated promoter control in addition to the IgG negative control. (B) EMSA using the 25 bp ZBP-89 binding site from the *CTNNB1* promoter at -120 bp upstream from the start site of transcription used as the WT probe (sense strand core consensus binding site for ZBP-89 in caps, <sup>-126</sup>tttccaccGCCCCtcgcgcgcccc); nucleotides mutated to A and T respectively are underlined (Mut). Lane 1: Probe; Lane 2: 6 µg nuclear extract; Lane 3: 100x molar excess of WT oligo; Lane 4: 100x molar excess of Mut oligo; Lane 5: 1µl Sp1 antibody (asterisks indicate Sp1 supershift); Lane 6: 1µl ZBP-89 antibody; Lane 7: 2µl ZBP-89 antibody; Lane 8: 3µl ZBP-89 antibody; Lane 9: 1µl each of Sp1 and ZBP-89 antibody. (C) DNA Affinity Precipitation Assay (DAPA) using the WT biotinylated probe. Lane 1: input nuclear extract; lane 2: precipitation with WT probe; lane 3: WT probe = 100× molar excess of WT oligo; lane 4: 100× molar excess with Mut oligo. Blotted with the ZBP-89 antibody. Nuclear extracts from SW480 cells used for both EMSA and DAPA. (D) Schematic of *ZNF148* cDNA expression vectors in pcDNA. Firefly luciferase assays normalized to Renilla after transfection of luciferase reporter pGL4, pcDNA or Full-length (FL) ZBP-89 expression plasmid. The *CTNNB1*

reporter plasmid (-591 to +147) without or with the 2-bp mutation at -120 (Mut) as described above transfected into SW480 or HEK293 cells (E, G). The *CTNNB1*-luciferase reporter co-transfected with full-length ZBP-89 or deletion constructs (FL ZBP-89,  $\Delta$ C-ter,  $\Delta$ Zinc Fingers) into SW480 or HEK293 cells (F, H). Bars represent the means of N= 5 experiments performed in triplicate  $\pm$ S.D. \*P<0.05; \*\*\*P<0.005, one-way ANOVA with Tukey's.

**Figure 6.  $\beta$ -catenin binds to the *ZNF148* promoter.** (A) Shows a schematic of the human *ZNF148* promoter with putative TCF/Lef binding sites identified. (B) PCR primers were used to amplify 3 regions of the promoter between -2197 and -606 bp upstream from the transcriptional start site following ChIP with  $\beta$ -catenin antibody. PCR products were analyzed on a 1% agarose gel. ChromograninA (CHRA) was used as an unrelated promoter control in addition to the IgG negative control. (C) PCR products precipitated with the antibody were analyzed by qPCR as a percent of the input. \*\*\*\*P<0.0001, one-way ANOVA with Tukey's. (D) Induction of *ZNF148* mRNA in SW480 cells by Wnt3A containing conditioned media in the presence of  $\beta$ -catenin and oncogenic  $\beta$ -catenin<sup>S33Y</sup>. Control = media from non-transfected L cells. N = 3 experiments in triplicate, \*P<0.05, \*\*P<0.01 relative to pcDNA vector control, one-way ANOVA with Tukey's.

**Figure 7. Feedforward regulation of  $\beta$ -catenin by ZBP-89.** Schematic summary suggesting that ZBP-89 sustains elevated levels of  $\beta$ -catenin in the normal crypt niche under homeostatic conditions and after loss of APC function.

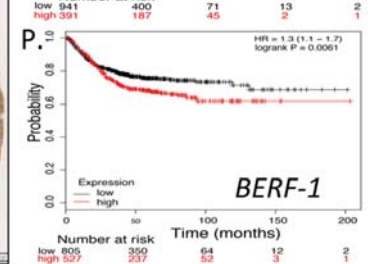
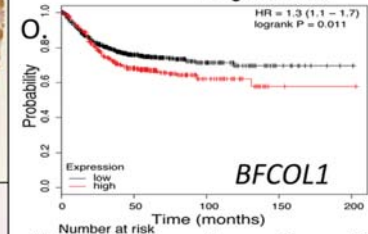
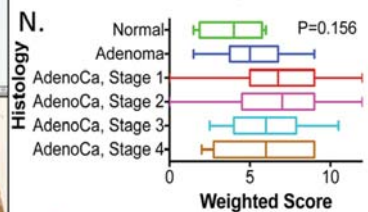
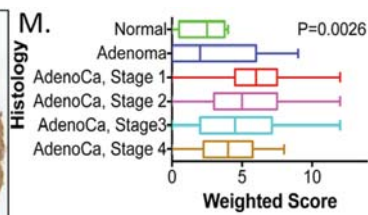
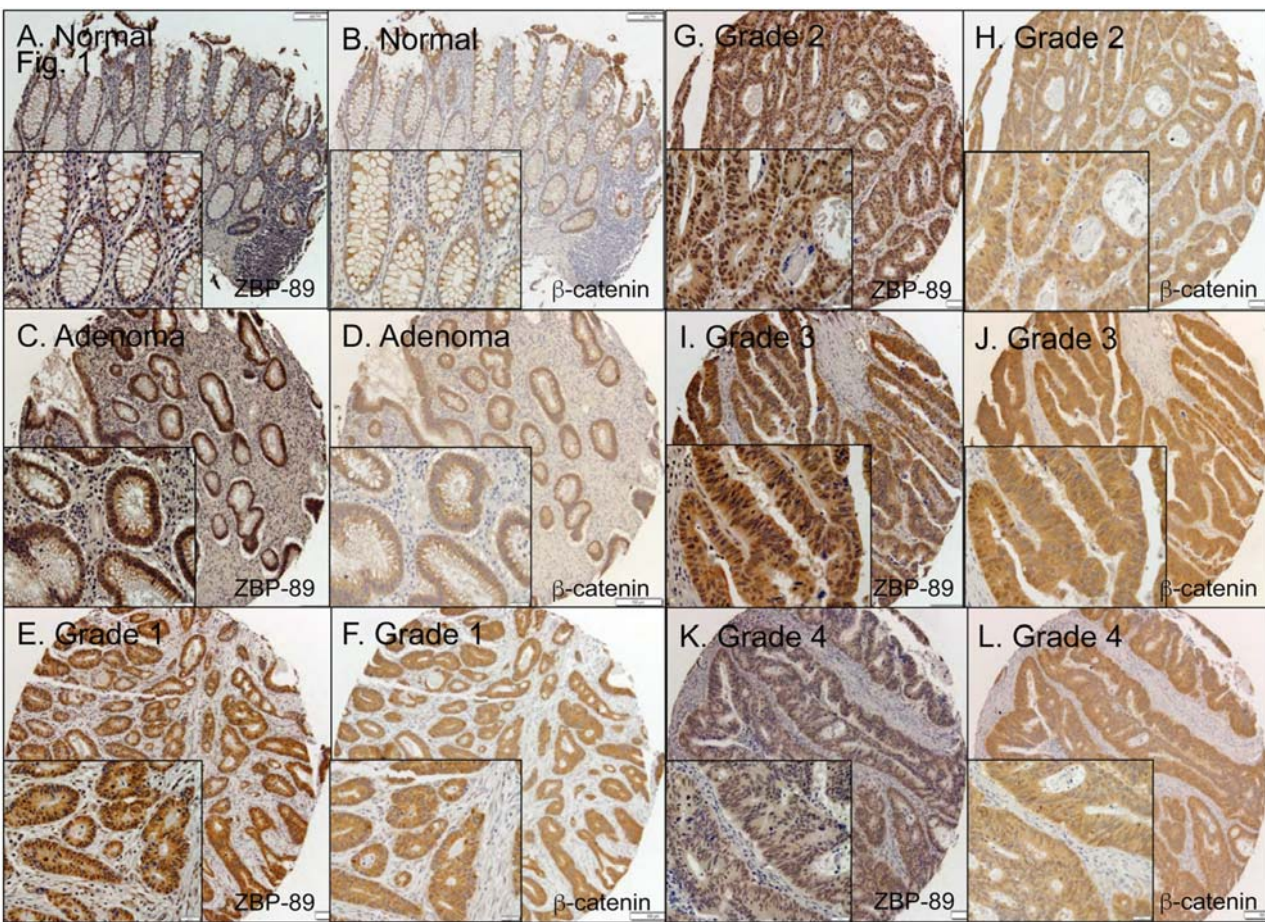


Fig. 2

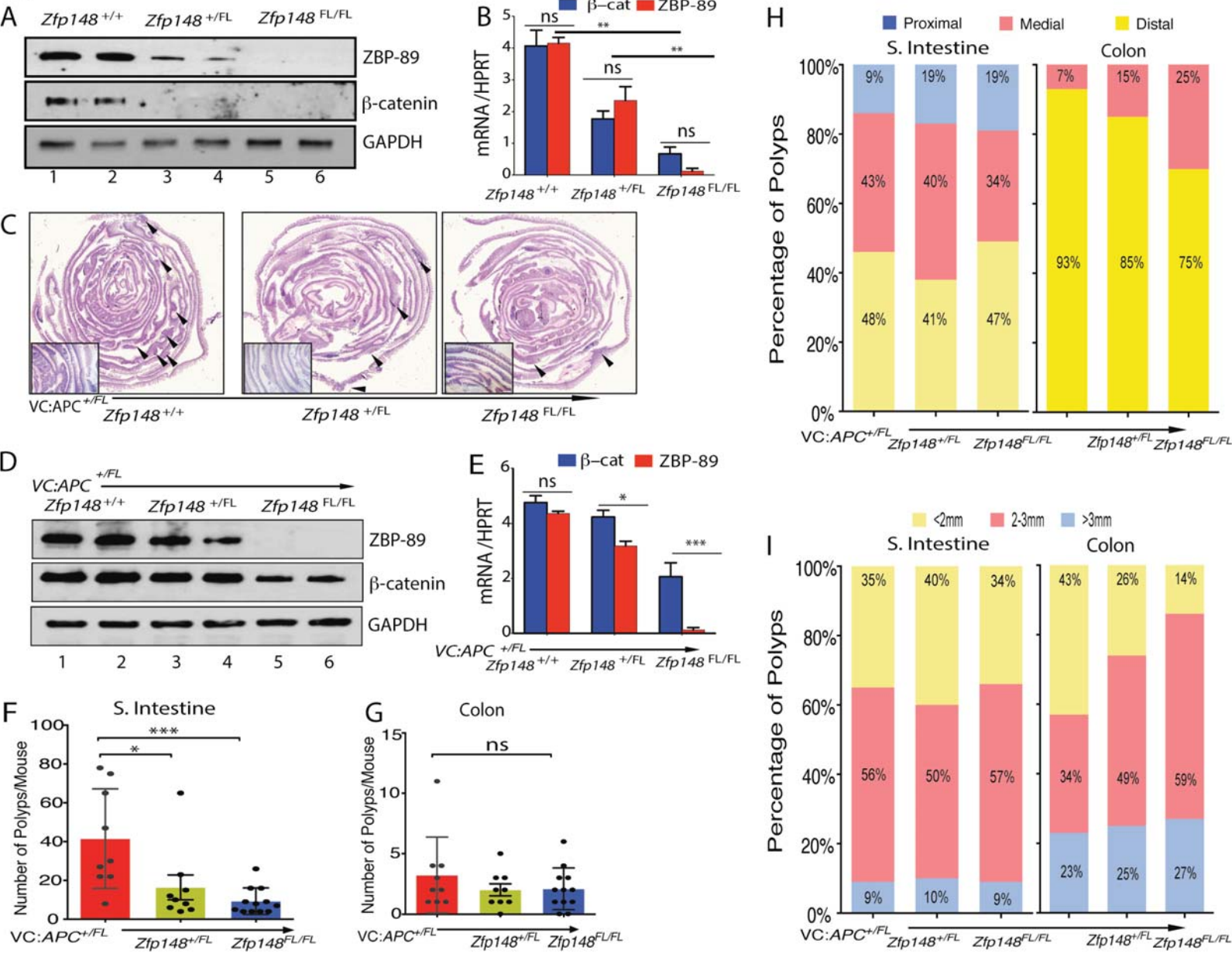




Fig. 3

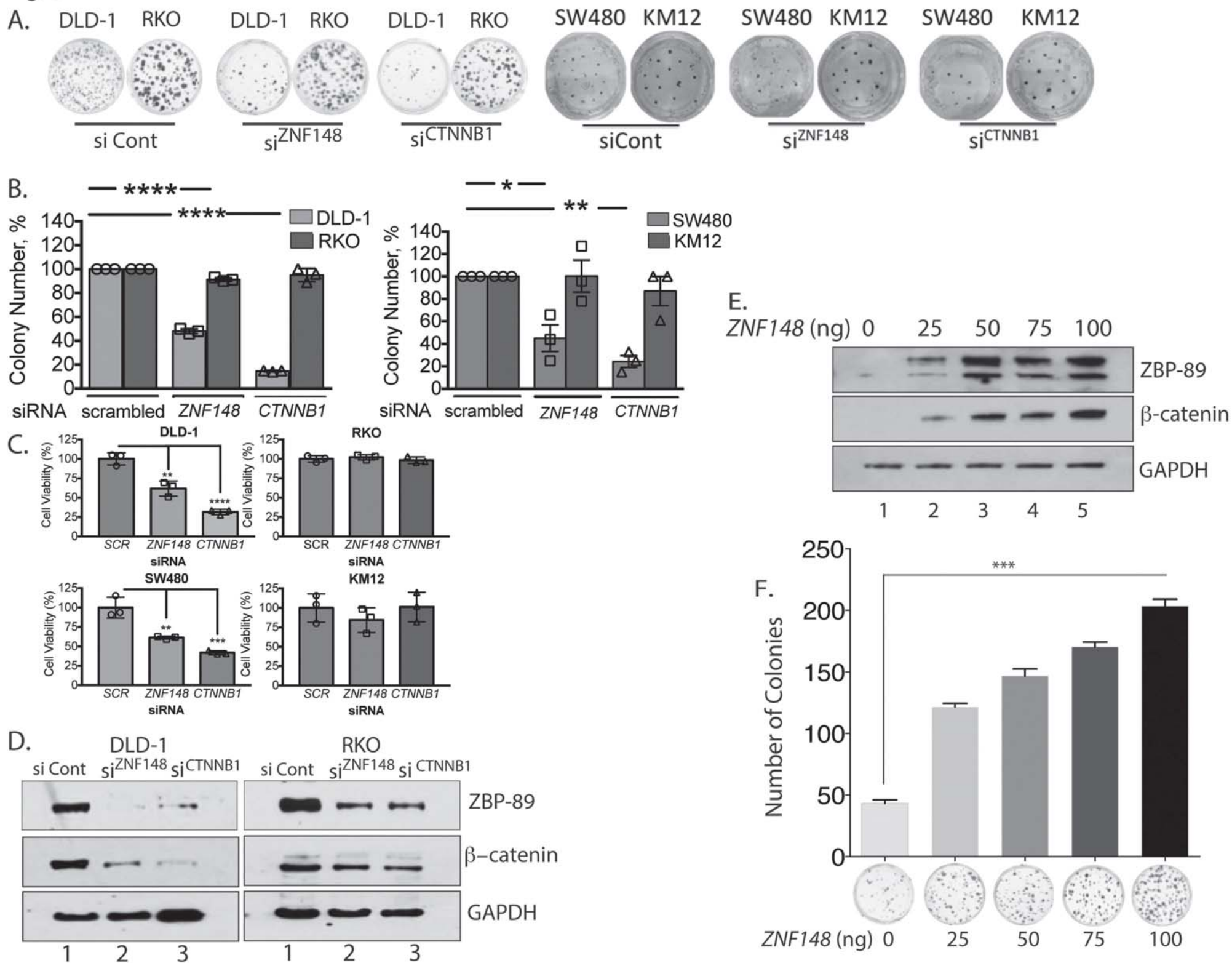
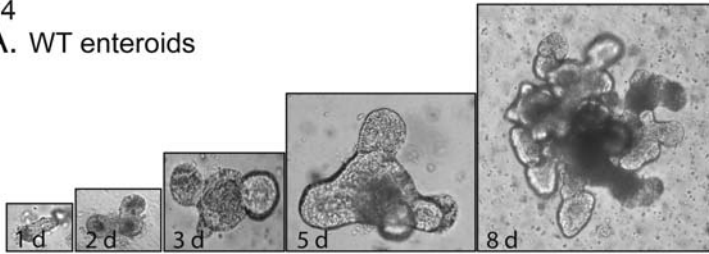
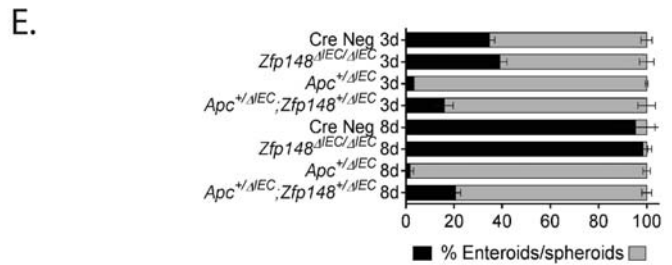
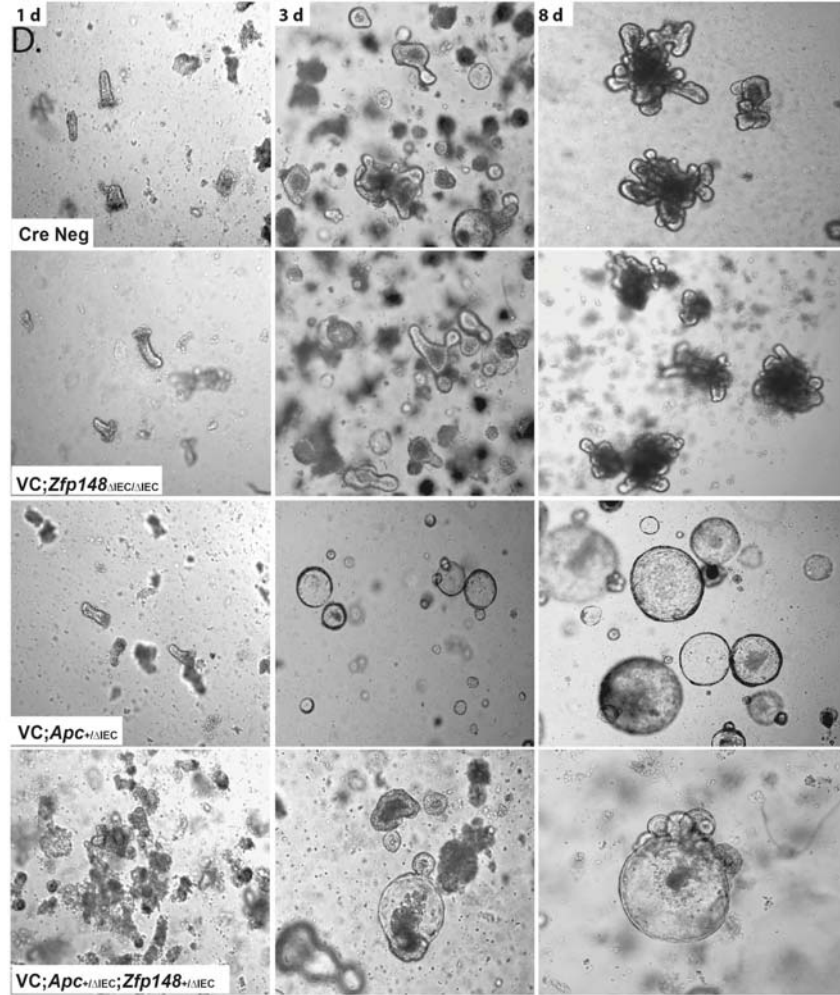
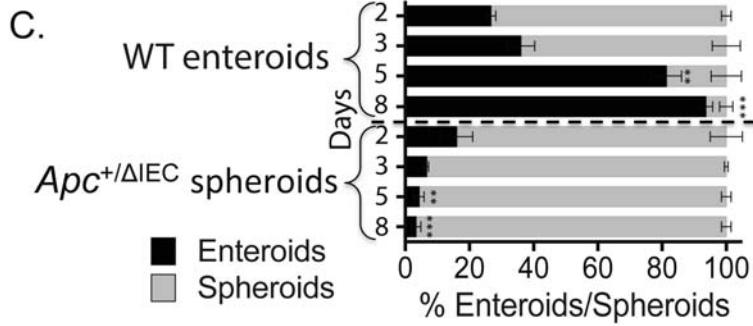
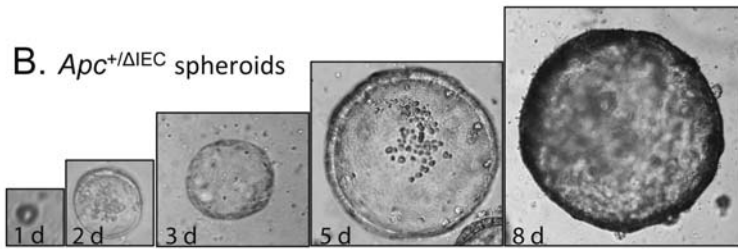


Fig. 4

A. WT enteroids



B. *Apc*<sup>+/ $\Delta$ IEC</sup> spheroids



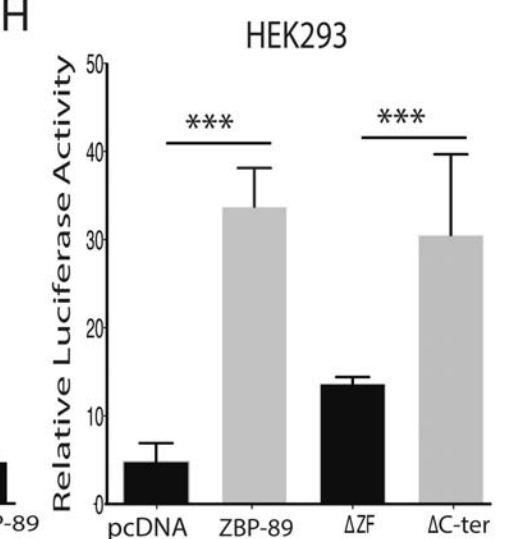
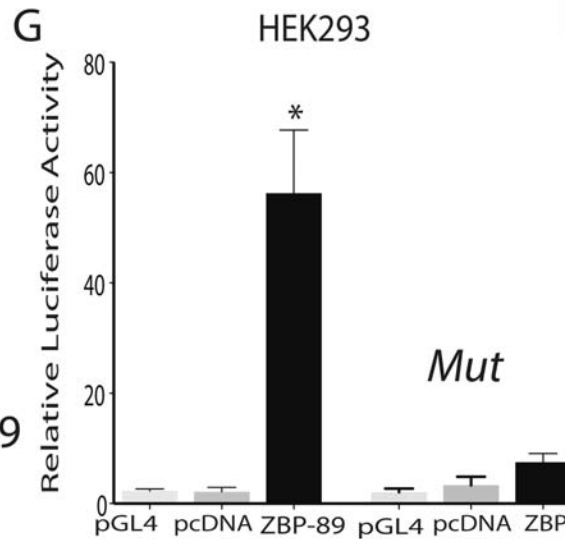
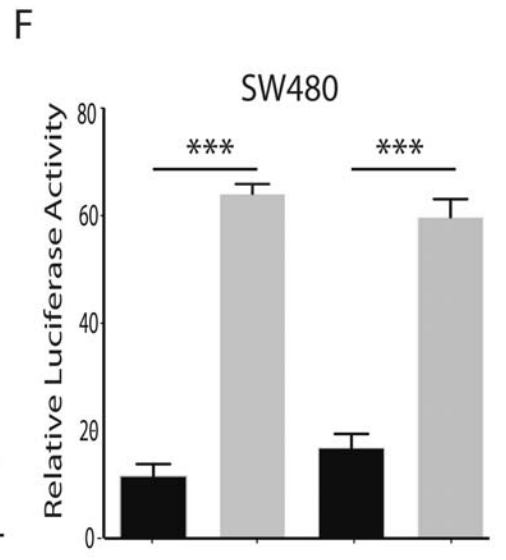
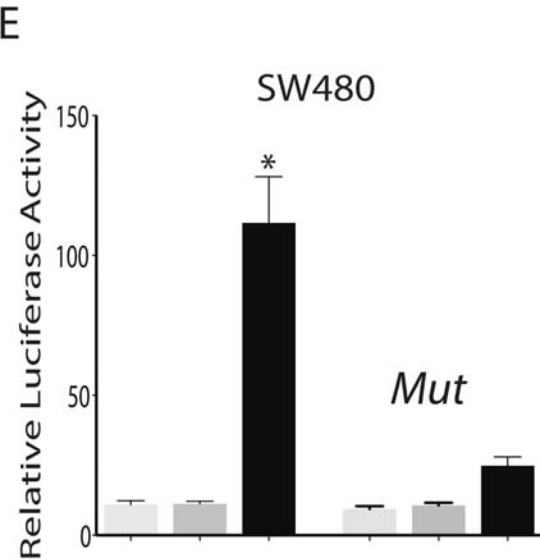
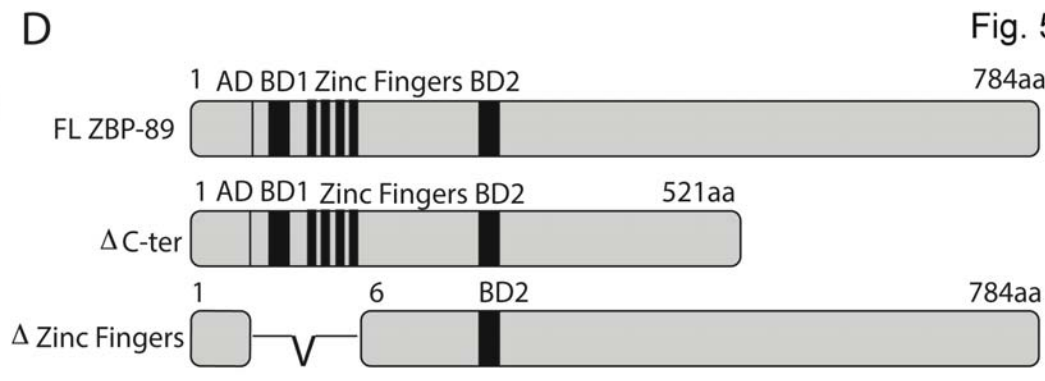
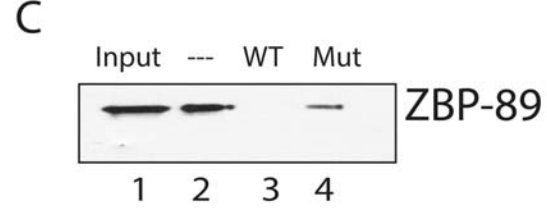
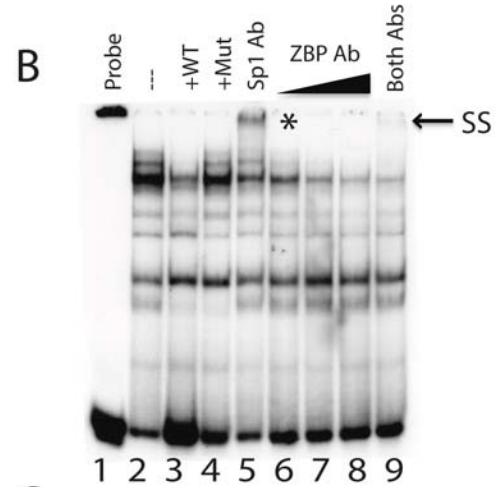
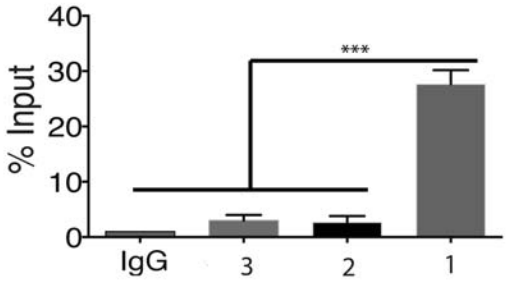
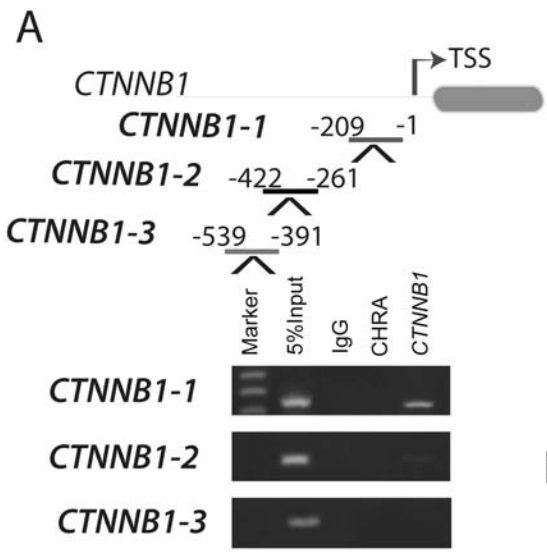


Fig. 6

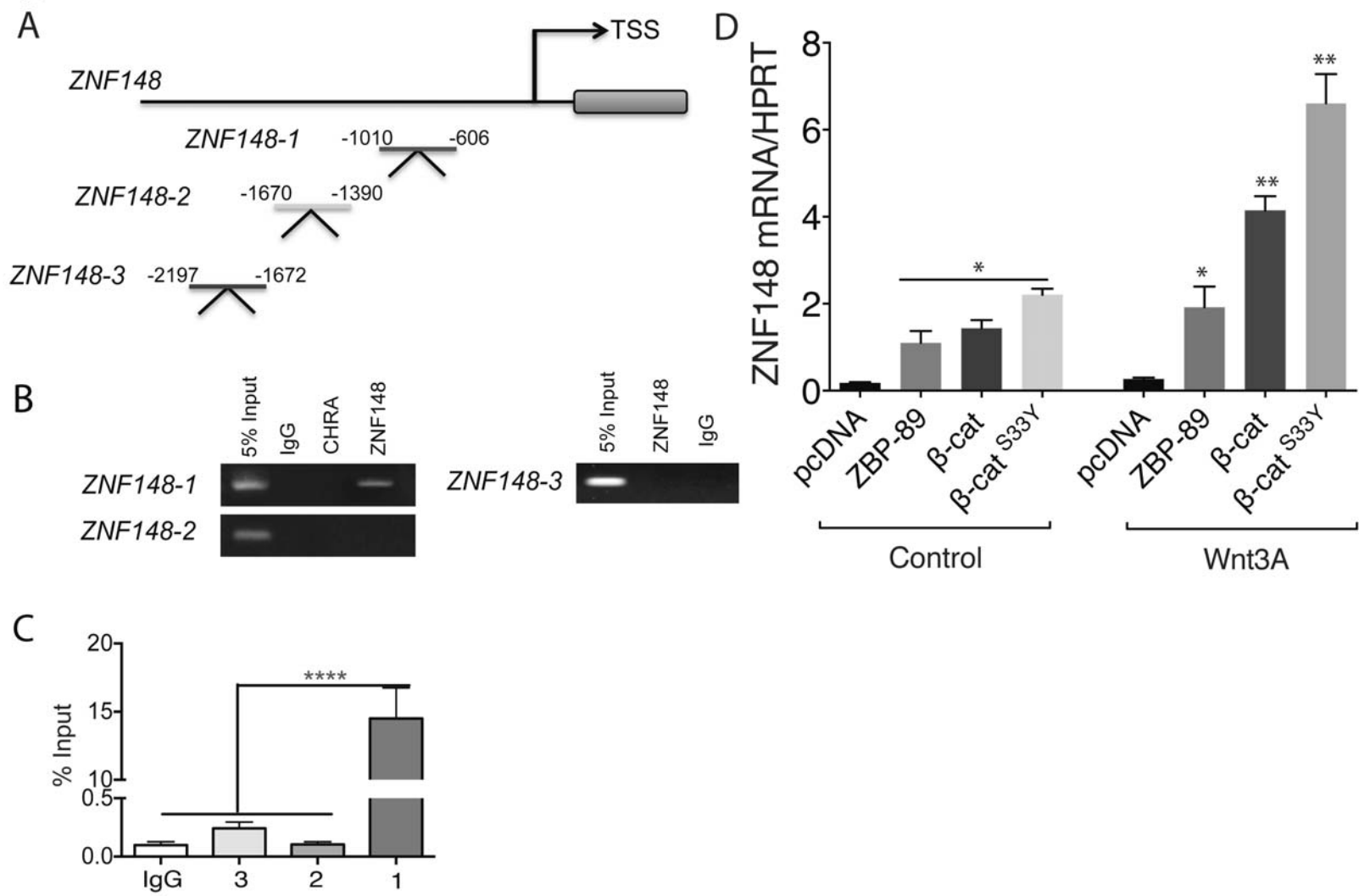


Figure 7

